

# Up-Regulation of miR-9-5p Inhibits Hypoxia-Ischemia Brain Damage Through the DDIT4-Mediated Autophagy Pathways in Neonatal Mice

Chengcheng Gai<sup>1,\*</sup>, Xiaohui Xing<sup>1,2,\*</sup>, Yan Song<sup>1</sup>, Yijing Zhao<sup>1</sup>, Zige Jiang<sup>1</sup>, Yahong Cheng<sup>1</sup>, Yilei Xiao<sup>1,2,3</sup>, Zhen Wang<sup>1,4</sup>

<sup>1</sup>Department of Physiology, School of Basic Medical Sciences, Cheeloo College of Medicine, Shandong University, Jinan, Shandong, 250012, People's Republic of China; <sup>2</sup>Department of Neurosurgery, Liaocheng People's Hospital, Liaocheng, Shandong, 252000, People's Republic of China; <sup>3</sup>Liaocheng Neuroscience Laboratory, Liaocheng People's Hospital, Liaocheng, Shandong, 252000, People's Republic of China; <sup>4</sup>Key Laboratory of Birth Regulation and Control Technology of National Health Commission of China, Maternal and Child Health Care Hospital of Shandong Province Affiliated to Qingdao University, Jinan, 250014, People's Republic of China

\*These authors contributed equally to this work

Correspondence: Yilei Xiao, Department of Neurosurgery, Liaocheng People's Hospital, Liaocheng, Shandong, 252000, People's Republic of China, Email yileixiao@163.com; Zhen Wang, Department of Physiology, School of Basic Medical Sciences, Cheeloo College of Medicine, Shandong University, 44 Wenhua Xi Road, Jinan, 250012, Shandong, People's Republic of China, Email wangzhen@sdu.edu.cn

**Introduction:** Hypoxia-ischemia (HI) remains the leading cause of cerebral palsy and long-term neurological sequelae in infants. Despite intensive research and many therapeutic approaches, there are limited neuroprotective strategies against HI insults. Herein, we reported that HI insult significantly down-regulated microRNA-9-5p (miR-9-5p) level in the ipsilateral cortex of neonatal mice.

**Methods:** The biological function and expression patterns of protein in the ischemic hemispheres were evaluated by qRT-PCR, Western Blotting analysis, Immunofluorescence and Immunohistochemistry. Open field test and Y-maze test were applied to detect locomotor activity and exploratory behavior and working memory.

**Results:** Overexpression of miR-9-5p effectively alleviated brain injury and improved neurological behaviors following HI insult, accompanying with suppressed neuroinflammation and apoptosis. MiR-9-5p directly bound to the 3' untranslated region of DNA damage-inducible transcript 4 (DDIT4) and negatively regulated its expression. Furthermore, miR-9-5p mimics treatment down-regulated light chain 3 II/light chain 3 I (LC3 II/LC3 I) ratio and Beclin-1 expression and decreased LC3B accumulation in the ipsilateral cortex. Further analysis showed that DDIT4 knockdown conspicuously inhibited the HI-up-regulated LC3 II/ LC3 I ratio and Beclin-1 expression, associating with attenuated brain damage.

**Conclusion:** The study indicates that miR-9-5p-mediated HI injury is regulated by DDIT4-mediated autophagy pathway and up-regulation of miR-9-5p level may provide a potential therapeutic effect on HI brain damage.

**Keywords:** hypoxia-ischemia, HI, miR-9-5p, DNA damage-inducible transcript 4, (DDIT4), autophagy

## Introduction

Hypoxia-ischemia (HI) is one of the leading causes of mortality and disability among neonates.<sup>1,2</sup> No satisfactory neuroprotective clinical treatment against HI has been identified. Mild hypothermia has been used as a routine treatment method for neonatal HI. Nevertheless, many infants still survive with disability after hypothermia treatment.<sup>3</sup> Therefore, there is an urgent need to advance our understanding of HI process and develop effective therapeutic strategies to rescue HI brain damage.

MicroRNAs (miRNAs), a novel family of non-protein coding short RNA molecules that negatively modulated protein expression, have been implicated in the particularly diagnostic and therapeutic tools for various diseases including HI

injury.<sup>4–7</sup> Previous studies demonstrated that miRNAs had been identified as crucial factors in modulating neuroinflammatory and other biological processes under HI brain damage.<sup>8,9</sup> MicroRNA-9 (miR-9) is a highly conserved across species and brain-enriched miRNA, which participates in regulating neuronal development.<sup>10</sup> MiR-9 assisted the proliferation and differentiation of neural progenitor in the developing brain by regulating the expression of multiple transcription factors.<sup>11,12</sup> MiR-9-5p levels were significantly reduced in a rat model of middle cerebral artery occlusion, while overexpression of miR-9-5p protected against ischemic brain injury by negatively regulating endoplasmic reticulum metalloprotease 1-induced inactivation of endoplasmic reticulum stress.<sup>13</sup> Furthermore, another study showed that miR-9-5p expression could regulate angiogenesis to limit neuronal VEGF-A signaling by targeting T cell leukemia homeobox and one cut homeobox.<sup>14</sup>

The DNA damage-inducible transcript (DDIT) 4 belongs to the DDIT or growth arrest DNA damage protein family that was known to have an essential role in regulating DNA damage repair, apoptosis, inflammatory response, neurodegenerative diseases.<sup>15–17</sup> Overexpression of DDIT4 promoted p38-mitogen-activated protein kinase pathway signaling and increased ROS overproduction to induce liver injury.<sup>18</sup> MiR-222-3p mediated the progression of neural tube defects by inhibiting DDIT4 to regulate the Wnt/ $\beta$ -catenin signaling pathway.<sup>19</sup> It is established that DDIT4 regulated autophagy through the mammalian target of rapamycin (mTOR)/autophagy axis and was involved in the progression of cancer, endocrine diseases and neurodegenerative diseases.<sup>20–22</sup>

In the present study, we found that the expression of miR-9-5p was significantly down-regulated after HI injury, and overexpression of miR-9-5p could attenuate inflammation and apoptosis to exert neuroprotective effects. Meanwhile, we proposed that miR-9-5p might target DDIT4 to regulate autophagy post-HI injury. Based on these results, miR-9-5p/DDIT4 may be a new promising treatment target for HI insult.

## Methods

### Neonatal Mice Model of Hypoxia-Ischemia

C57BL/6J mice used in all experiments were provided by the Charles River Laboratory Animal Technology Co., Ltd. (Beijing, China). The ethics approval statements for animal work and procedures were approved by the Institutional Animal Care and Use Committee of Shandong University (approval No. ECSBMSSDU2018-2-059) (Shandong, China). The entire experimental process followed the “Guiding Opinions on the Good Treatment of Laboratory Animals” issued by the Ministry of Science and Technology of the People’s Republic of China. The HI model in neonatal mice was established according to the Rice-Vannucci method<sup>23</sup> which simulates neonatal encephalopathy in term infants. In brief, at postnatal day (PND) 7, mice were anesthetized with isoflurane and a vertical incision was made in the neck. The right common carotid artery was permanently ligated with prolene sutures. After 30 min of postsurgical recovery, mice were subjected to hypoxia (9.7% O<sub>2</sub>/90.3% N<sub>2</sub>, 5% CO<sub>2</sub>) at 37°C for 1 h. After hypoxia, the pups were returned to their dam until sacrifice. Sham was anesthetized with isoflurane on PND 7, and the right common carotid artery was separated but not ligated.

### Intracerebroventricular (i.c.v.) Treatment

PND 4 mouse pups were fixed in prone position under isoflurane anesthesia. Insert the needle 3 mm deep, perpendicular to the skull surface, at a location midpoint of lambda and bregma sutures and approximately 1 mm lateral to the sagittal suture.<sup>24</sup> Then  $1 \times 10^8$  TU/mL (3  $\mu$ L) of miR-9-5p mimics or negative control (NC), 2  $\mu$ g/ $\mu$ L (3  $\mu$ L) DDIT4 vector or overexpression plasmid were injected into the lateral ventricle. The injection rate was 1  $\mu$ L/2 min, and we waited for about 5 min after the injection was completed. Neonates were placed back on the heating pad until they had recovered their locomotion and general response, and then neonates were placed back in their cages.

### Infarct Area Measurement

Animals were transcardially perfused with phosphate buffered sodium (PBS) under deep anesthesia 2 days post-HI. The brains were kept at  $-20^{\circ}\text{C}$  for 10 min and then sectioned into 2 mm slices. The infarct area was examined by 2% 2, 3,

5-triphenyltetrazolium chloride (TTC, Sigma, St Louis, USA) in PBS at 37°C for 20 min. The infarct area was determined by ImageJ software.

$$\text{Infarct area(\%)} = \frac{\text{contralateral hemisphere area} - \text{healthy areas of the ipsilateral hemisphere}}{\text{contralateral hemisphere area}} \times 100\%$$

## Immunofluorescence and Immunohistochemistry Staining

Tissue sections were deparaffinized in xylene and then rehydrated in graded alcohol of 100%, 95% and 75%. After blocked with 5% normal goat serum for 1 h at room temperature, slides were incubated with primary antibody at 4 °C overnight. Wash steps were performed and the sections were incubated with secondary antibodies. Immunofluorescence sections were counterstained with 4,6-diamino-2-phenyl indole (DAPI) for 10 min. Finally, the slides were visualized under a microscope (Olympus, Tokyo, Japan). There were three mice in each experimental group and two sections per mouse were randomly selected for imaging. The number of positive cells was calculated the numbers in six images from each mouse. Counting was performed in a blinded manner.

Tissue sections were deparaffinized in xylene and then rehydrated in graded alcohol of 100%, 95% and 75%. The endogenous peroxidase activity was inhibited by incubation of the slide for 30 min in 0.3% H<sub>2</sub>O<sub>2</sub> in 0.01 mol/L Tris. Visualization was achieved with peroxidase-labeled streptavidin-biotin and diaminobenzidine (Gene Tech, Shanghai, China) for at least 1 min in immunohistochemistry slide, and the sections were re-stained with hematoxylin. Finally, the slides were visualized under a microscope (Olympus). There were three mice in each experimental group and two sections per mouse were randomly selected for imaging. Three 200× fields of image were randomly selected in each section for counting. Counting was performed in a blinded manner. Activated microglia scores were assigned as previously described.<sup>25</sup> Semi-quantitative scores for Iba-1 staining were present in [Table 1](#).

## Luciferase Reporter Assay

To explore miR-9-5p binding to the DDIT4 3' untranslated region (3'UTR), DDIT4 mutant type sequences (DDIT4-Mut) and DDIT4 wild type sequences (DDIT4-WT) were cloned into luciferase reporter of pMIR, respectively. HEK239T cells were seeded in 24-well plates and transfected with miR-9-5p NC, miR-9-5p mimics, DDIT4-Mut and DDIT4-WT. After 2 days, the cells were lysed in passive lysis buffer for 15 min. After that, Firefly/Renilla luciferase activity was extracted using the dual-luciferase reporter assay system (Promega, Madison, USA) according to the manufacturer's instructions.

## TUNEL Assay

Detection of apoptosis was performed according to the manufacturer's instructions (Servicebio, Wuhan, China). Paraffin section were dewaxed and hydrated by alcohol gradient. The slices were incubated with protease K at 25°C for 30 min to remove tissue proteins. Sections were incubated in the TUNEL reaction mixture containing the marking solution (2'-deoxyuridine 5'-triphosphate-dUTP+fluorescein isothiocyanate-conjugated-FITC) with enzymatic solution (terminal deoxynucleotidyl transferase) for 1 h in a humidified chamber at 37°C in the dark. Samples were then washed and stained with DAPI for 10 min, washed with PBS and sealed. Finally, the slides were visualized under a microscope.

**Table 1** Semi-Quantitative Scores for Iba-1 Staining

Score	Microglial Appearance
0	No activation
1	Foci of non-ramified active microglia
2	<50% coverage of active microglia
3	Widespread active and predominantly phagocytic microglia
4	Total phagocytic activation

## Y-Maze Test

Y-maze test was used to measure working memory. Y-maze testing was performed using an apparatus with three equal arms at a 120-degree angle. Arm entry was defined as the entry of all four paws into the arm. Mice were allowed to freely explore the two open arms (“start arm” and “other arm”) in training phase for 5 min. During the testing period mice could explore all arms in the maze for 5 min. The number of entries into the novel arm was recorded and analyzed by Smart 2.5 digital tracking system (Panlab, Barcelona, Spain).

## Open Field Test

The open field test was used to estimate locomotor activity and exploratory behavior. Mice were placed near the wall of a 40×40 cm open field arena and allowed to explore the open field for 5 min. Each mouse was placed in the central field at the start of the test. The trajectory of mice was monitored for 5 min using a camera. The crossing number, grooming number, feces number and rearing number were recorded.

## Western Blotting Analysis

Proteins were isolated from brain tissue samples and lysed in RIPA. Concentration of protein was determined by BCA protein assay kit (Cwbio, Beijing, China). The proteins were separated by SDS-PAGE, and transferred to a polyvinylidene difluoride (PVDF) membranes (Millipore, MA, USA). PVDF membranes were blocked with 5% non-fat dried milk, and incubated at 4°C overnight with primary antibodies: Arginase-1 (Arg-1) (9819; Cell Signaling Technology), Beclin-1 (3495; Cell Signaling Technology), caspase-3 (19677-1-AP; Proteintech), cleaved caspase-3 (9661, Cell Signaling Technology), inducible nitric oxide synthase (iNOS) (18985-1-AP; Proteintech), IL-1 $\beta$  (sc-7884; Santa Cruz), light chain 3 B (LC3B) (2775; Cell Signaling Technology), neuroligin (NLG)-1 (ab186279; Abcam), postsynaptic density-95 (PSD95) (3409; Cell Signaling Technology), and  $\beta$ -actin (TA-09, Zhongshan Golden Bridge Biotechnology). Secondary antibodies were applied and the signals were detected by enhanced chemiluminescence (Millipore, MA, USA). Semi-quantification of the blots was calculated by Image J software.

## Quantitative Real-Time Polymerase Chain Reaction (qRT-PCR) Assay

Total RNAs were extracted using Ultrapure RNA Kit (Cwbio, Beijing, China). RNA was reversed transcribed following Revert Aid First Strand cDNA Synthesis Kit (TOYOBO, Osaka, Japan) according to manufacturer’s protocol. The qRT-PCR was performed on the Bio-rad IQ5 Real Time PCR System (Bio-Rad, CA, USA) using SYBR Green PCR master mix (Aidlab Biotechnologies, Beijing, China). The mRNA levels were normalized to GAPDH or U6 levels. The primer sequences were as follows: B-cell translocation gene 1 (BTG2): F: 5'-CCCCCGGTGGCTGCCTCCTATG-3' and R: 5'-GGGTCGGGTGGCTCCTATCTA-3'; CXC ligand 12 (CXCL12): F: 5'-TGCATCAGTGACGGTAAACCA-3' and R: 5'-TGTCTGTGTGTTCTTCAGCCGTGC-3'; CXC chemokine receptor 4 (CXCR4): F: 5'-TGCAGCAGGTAGCAGTGAAA-3' and R: 5'-AAGTGTATACTGATCGGTTCCA-3'; DDIT4: F: 5'-GTGCTGCGTCTGGACTCTC-3' and R: 5'-CCGGTACTTAGCGTCAGGG-3'; Furin: F: 5'-CAGAAGCATGGCTTCCACAAC-3' and R: 5'-TGTCAGTCTGTGCCAGAA-3'; miR-9-5p: F: 5'-AGCCTCTCTCCTCTTTGGTTATCT-3' and R: 5'-TATGGTTGTTCTGCTCTCTGTGTC-3'; GAPDH: F: 5'-ATACGGCTACAGCAACAGGG-3' and R: 5'-GCCTCTCTGCTCAGTGTCC-3'; U6: F: 5'-CAGCACATATACTAAAATTGGAACG-3' and R: 5'-ACGAATTTGCGTGTATCC-3'.

## Statistical Analysis

All data were expressed as mean $\pm$ SD. Quantifications were performed using at least three independent experimental groups. Statistical differences between two experimental groups were analyzed by a two-tailed Student’s *t*-test. Multiple comparisons were analyzed with one way ANOVA followed by the Bonferroni corrections. Differences were considered statistically significant when  $p < 0.05$ .

## Results

### Exogenous miR-9-5p Treatment Attenuated Brain Damage After HI Insult

We detected the level of miR-9-5p expression in the ipsilateral cortex at 0 day to 7 days after HI using qRT-PCR. Levels of miR-9-5p expression were decreased at 1 day ( $p < 0.05$ ), 2 days ( $p < 0.001$ ), 3 days ( $p < 0.01$ ) and 7 days ( $p < 0.01$ ) following HI insult (Figure 1A). Moreover, the level of miR-9-5p expression in the ipsilateral cortex was significantly increased after i.c.v. of miR-9-5p mimics ( $p < 0.001$ ) (Figure 1B). To investigate whether the up-regulation of miR-9-5p could mitigate brain damage in vivo, we examined brain damage at 2 days post-HI with miR-9-5p NC or miR-9-5p mimics treatment. HI+miR-9-5p mimics group could alleviate HI-induced edema compared to HI+miR-9-5p NC group (Figure 1C). According to the quantitative analysis of the TTC-stained sections, miR-9-5p mimics treatment effectively reduced infarct area ( $p < 0.01$ ) (Figure 1D and E). In addition, TUNEL staining showed that miR-9-5p mimics treatment attenuated cell apoptosis in the ipsilateral cortex at 2 days after neonatal HI (Figure 2A). Moreover, cleaved caspase-3/caspase-3 ratio in the ipsilateral cortex decreased in HI+miR-9-5p mimics group ( $p < 0.001$ ) compared to HI+miR-9-5p NC group (Figure 2B and C).

### Effects of miR-9-5p on Microglial Morphological Alterations and Cytokines Expression Following HI Insult

We used immunohistochemistry to detect the alterations of microglia morphology in the ipsilateral cortex following HI exposure. HI exposure increased the level of Iba-1<sup>+</sup> cells ( $p < 0.001$ ) and microglia/macrophage activation scores ( $p < 0.001$ ) in the ipsilateral cortex compared with Sham group (Figure 3A–C). Nevertheless, miR-9-5p mimics treatment

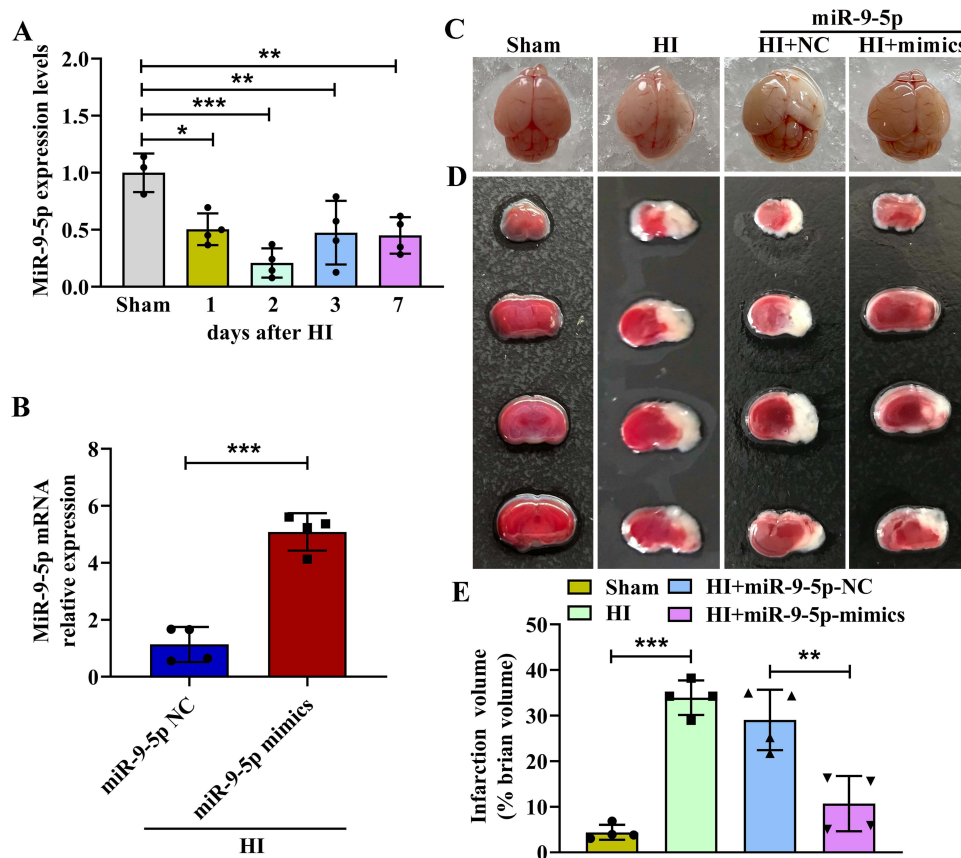


**Figure 1** MiR-9-5p expression was decreased post HI and overexpression of miR-9-5p could ameliorate brain injury. (A) The expression levels of miR-9-5p mRNA were detected by qRT-PCR at 0 to 7 days after HI injury. (B) The expression levels of miR-9-5p mRNA were measured after HI with miR-9-5p mimics treatment. (C and D) Representative pictures of the brain and TTC staining of the brain. (E) Quantification of brain infarct area in each group. The data were presented as mean  $\pm$  SD. \* $p < 0.05$ , \*\* $p < 0.01$ , \*\*\* $p < 0.001$  according to One-way ANOVA with Dunnett corrections in (A); \*\*\* $p < 0.001$  according to t-test in (B); \*\* $p < 0.01$ , \*\*\* $p < 0.001$  according to One-way ANOVA with Bonferroni corrections in (E).

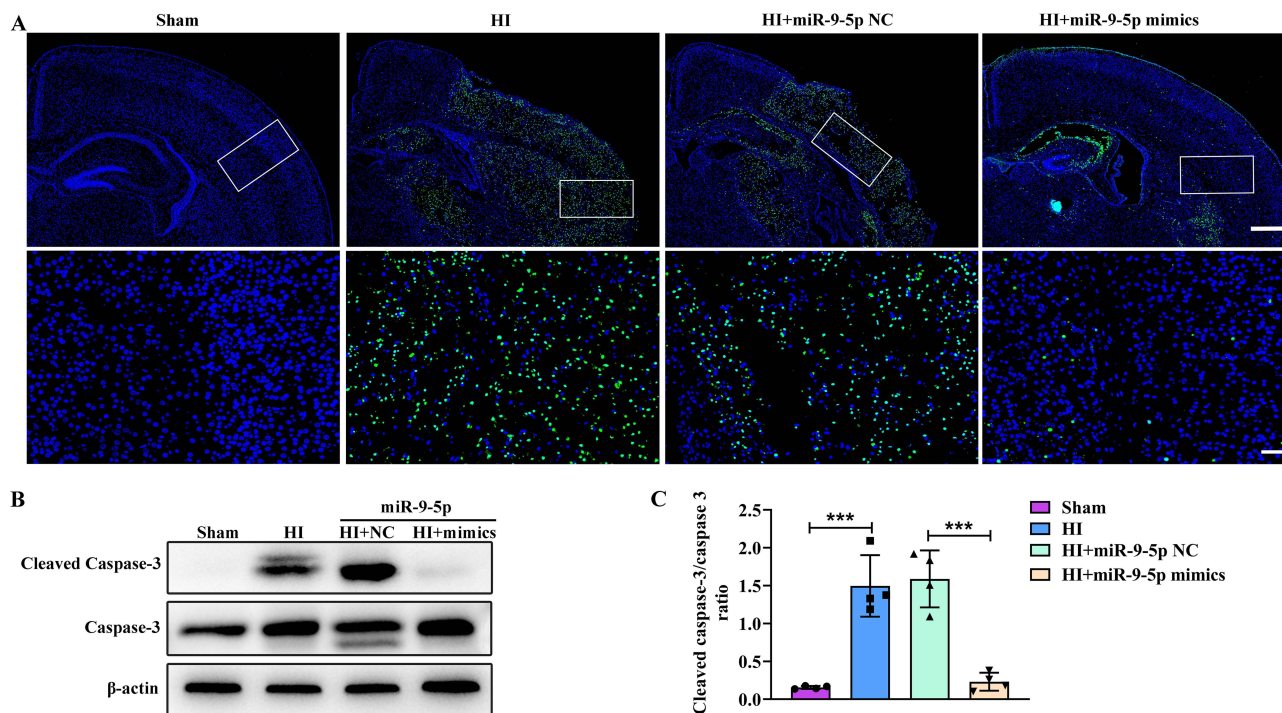


**Figure 2** MiR-9-5p alleviated apoptosis after HI injury. **(A)** TUNEL assay to detect apoptotic in Sham group, HI group, HI+miR-9-5p NC group and HI+miR-9-5p mimics group. Scale bar: 400  $\mu$ m. Magnified views of boxed regions scale bar: 50  $\mu$ m. **(B and C)** The expression levels of cleaved caspase-3 and caspase-3 protein were analyzed by Western blotting. The data were presented as mean  $\pm$  SD, \*\*\* $p$  < 0.001 according to One-way ANOVA with Bonferroni corrections in **(C)**.

reversed decreased the level of Iba-1<sup>+</sup> cells ( $p$  < 0.001) and microglia/macrophage scores ( $p$  < 0.001) (Figure 3A–C). Furthermore, the level of Arg-1 protein expression was increased in HI+miR-9-5p mimics group ( $p$  < 0.05). However, levels of iNOS ( $p$  < 0.001) and IL-1 $\beta$  ( $p$  < 0.001) protein expression were significantly decreased in HI+miR-9-5p mimics group (Figure 3D and E).

## Effect of miR-9-5p on Brain Atrophy and Synaptic Relative Proteins

Extensive atrophy of ipsilateral brain tissue was observed at 28 days ( $p$  < 0.001) post-HI, while i.c.v. of miR-9-5p mimics significantly reduced brain atrophy ( $p$  < 0.001) compared to the miR-9-5p NC group (Figure 4A and B).

The expression levels of PSD95 and NLG-1 were evaluated by Western blotting. The results showed that PSD95 and NLG-1 protein levels were significantly reduced at 2 days (PSD95:  $p$  < 0.001 and NLG-1:  $p$  < 0.001) and 28 days (PSD95:  $p$  < 0.001 and NLG-1:  $p$  < 0.001) after HI injury (Figure 5A–D). MiR-9-5p mimics treatment significantly increased the expression levels of PSD95 and NLG-1 protein in comparison to miR-9-5p NC at 2 days (PSD95:  $p$  < 0.05 and NLG-1:  $p$  < 0.001) and 28 days (PSD95:  $p$  < 0.001 and NLG-1:  $p$  < 0.001) after HI injury (Figure 5A–D). Compared with the Sham group, the results of immunofluorescence double staining showed that the number of PSD95<sup>+</sup>/NeuN<sup>+</sup> neurons was significantly decreased ( $p$  < 0.001) at 28 days post HI, while miR-9-5p mimics treatment was able to increase the number of PSD95<sup>+</sup>/NeuN<sup>+</sup> neurons ( $p$  < 0.001) in the ipsilateral cortex (Figure 5E).

## Effects of miR-9-5p on Neurobehavioral Impairment Following HI Injury

We next performed open field test and Y-maze test at 28 days after HI injury to explore the effects of miR-9-5p on neurological deficits. As shown in Figure 6A, the motor activity of the HI group was significantly increased compared to the Sham group, which was represented by the crossing number ( $p$  < 0.05). While there were no difference in grooming, feces and rearing number. Furthermore, miR-9-5p mimics treatment significantly reduced the crossing number ( $p$  < 0.05) in HI-injured mice (Figure 6A). The results of the Y maze test showed that overexpression of miR-9-5p reversed the HI-induced working memory deficit, as evidenced by a significant reduction in the number of mice entries into the novel arm

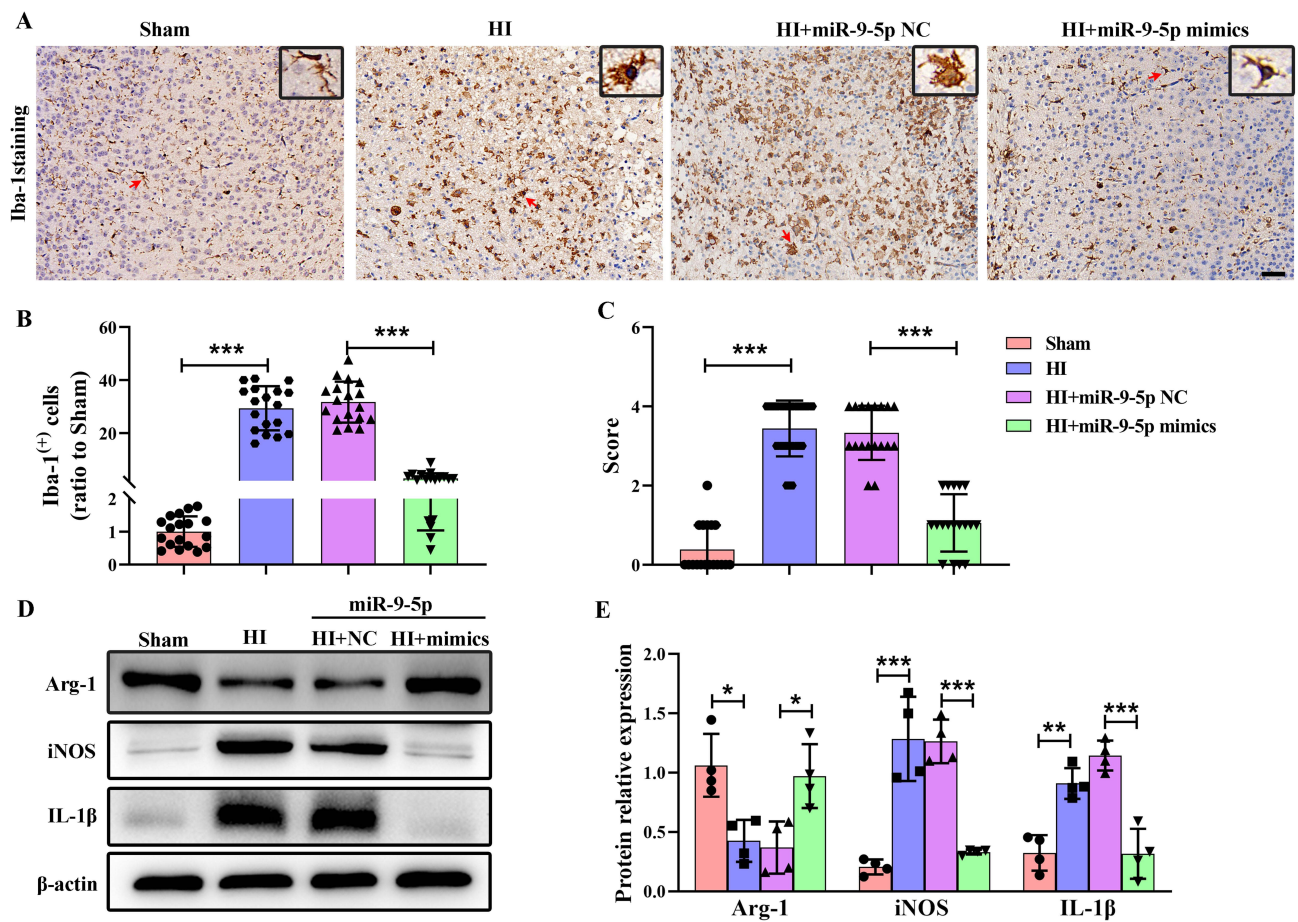


**Figure 3** MiR-9-5p inhibited inflammatory activation after HI injury. **(A)** Representative images of Iba-1 immunohistochemical staining at 2 days following HI insult. Scale bar: 50  $\mu$ m. Red arrow: microglia/macrophages. Magnified views of black box regions in A shows morphology of microglia/macrophages indicated by red arrow. **(B)** Quantification of Iba-1<sup>+</sup> cells in the Sham group, HI group, HI+miR-9-5p NC group and HI+miR-9-5p mimics group. **(C)** Quantitative analysis of the effect of miR-9-5p on microglia/macrophage activation scores. **(D and E)** Western blotting was detected protein expression levels of iNOS, IL-1 $\beta$  and Arg-1 at 2 days post HI. The data were presented as mean  $\pm$  SD, \* $p$  < 0.05, \*\* $p$  < 0.01, \*\*\* $p$  < 0.001 according to One-way ANOVA with Bonferroni corrections in **(B, C and E)**.

( $p$  < 0.05) (Figure 6B). These data demonstrated that up-regulation of miR-9-5p expression could ameliorate HI-induced neurobehavioral outcomes at 28 days after HI.

## DDIT4 as a Target Gene of miR-9-5p Post-HI Injury

To elucidate the target mechanisms by which miR-9-5p mimics elicits protective response to HI insult, we first predicted the potential target genes of miR-9-5p using miRNAs relative databases (TargetScan, PicTar-Vert, and MiRanda). We screened BTG2, FURIN, CXCL12, CXCR4 and DDIT4 as possible downstream target genes of miR-9-5p. Next, we examined the expression changes of their mRNA after HI injury and treatment with miR-9-5p mimics. The results showed that CXCL12 ( $p$  < 0.05) and DDIT4 ( $p$  < 0.01) expression was up-regulated at 2 days after HI injury and DDIT4 mRNA ( $p$  < 0.01) level could be suppressed by miR-9-5p mimics treatment. However, CXCL12 mRNA level had no significant difference between HI+miR-9-5p mimics group and HI+miR-9-5p NC group (Figure 7A). Consequently, DDIT4 was identified as a candidate of a downstream target of miR-9-5p in the present study. Luciferase reporter vector containing the 3'UTR fragment of DDIT4 encompassing the miR-9-5p binding sites or a mutated fragment were constructed and transfected into HEK293T cells (Figure 7B). We found that miR-9-5p significantly inhibited the luciferase activity of the vector containing the DDIT4-WT ( $p$  < 0.001) binding site, whereas it failed to affect the luciferase activity elicited by the DDIT4-MUT construct (Figure 7C), suggesting that miR-9-5p repressed DDIT4 by binding to the 3'UTR of this gene. SiRNA targeting DDIT4 (si-DDIT4) was infected into HI-injured mice to knockdown DDIT4 level ( $p$  < 0.01). DDIT4 overexpression plasmid was infected into Sham and HI-injured mice to upregulate

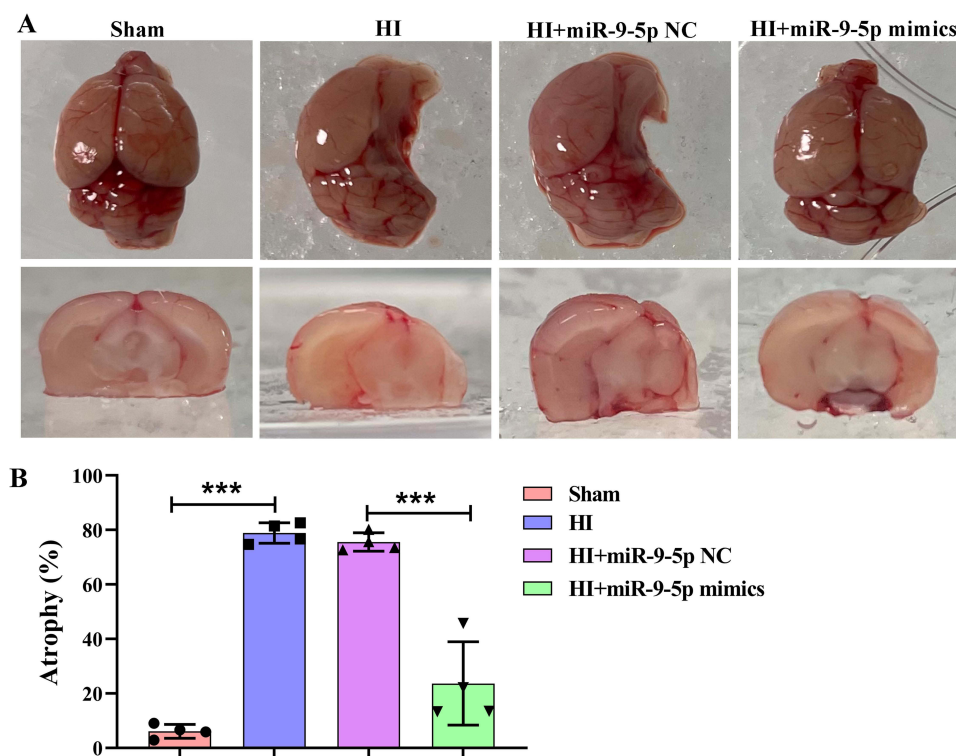


**Figure 4** The effect of miR-9-5p on brain atrophy at 28 days after HI. **(A)** Representative images of brain atrophy at 28 days after HI insults. **(B)** Quantitative analysis of brain atrophy area in Sham group, HI group, HI+miR-9-5p NC group and HI+miR-9-5p mimics group. The data were presented as mean  $\pm$  SD, \*\*\* $p$  < 0.001 according to One-way ANOVA with Bonferroni corrections in **(B)**.

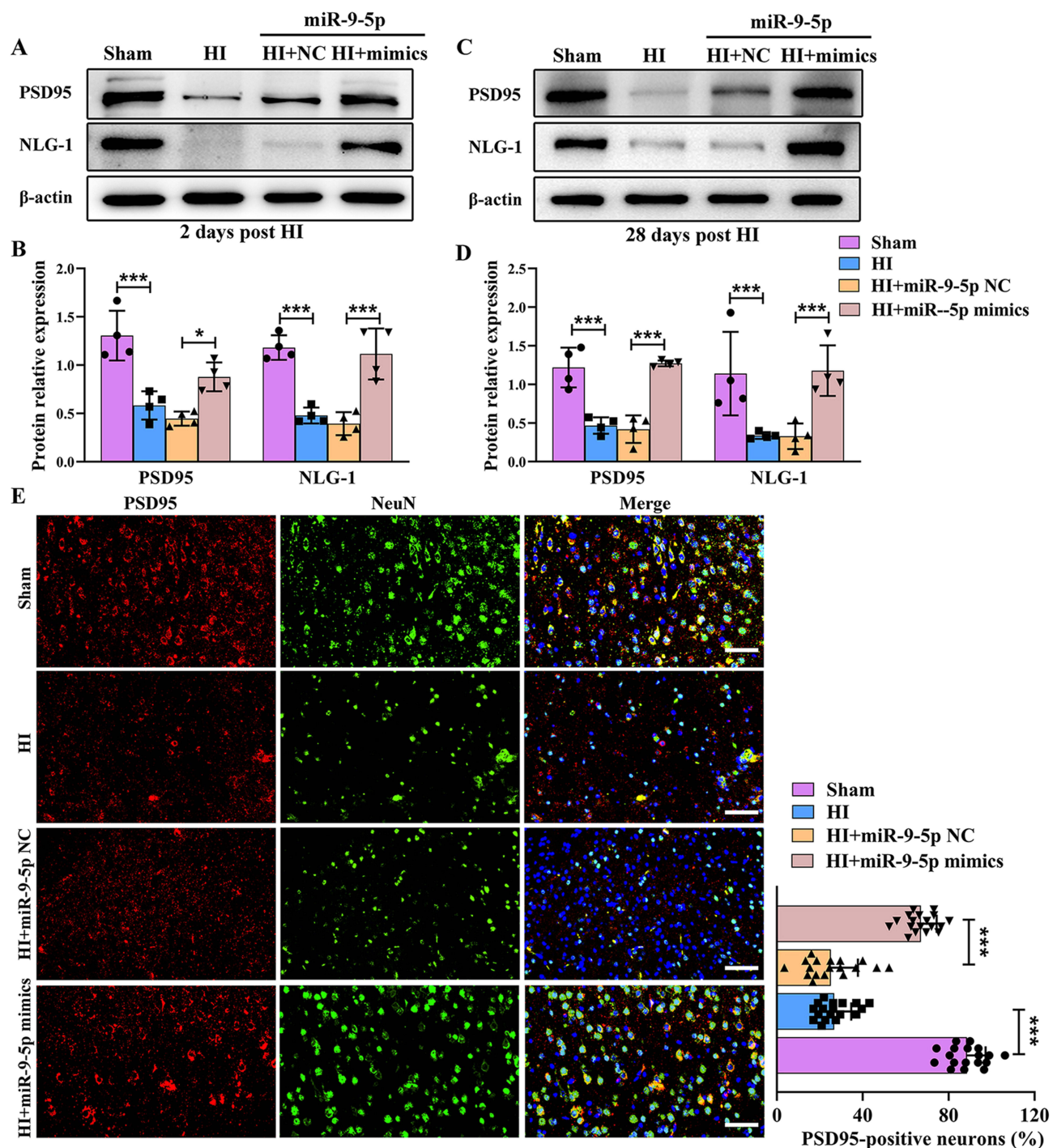
DDIT4 level ( $p$  < 0.01,  $p$  < 0.05, respectively) (Figure 7D). Interestingly, DDIT4 knockdown suppressed HI-induced brain edema and cerebral infarction ( $p$  < 0.001). Overexpression of DDIT4 reversed the effect of miR-9-5p mimics on HI-induced edema and infarction ( $p$  < 0.001) (Figure 7E–G).

## Effects of miR-9-5p on HI-Induced Autophagosome Formation

It has been reported that DDIT4 negatively regulates the mTOR-dependent autophagy in ischemia animals.<sup>26,27</sup> Therefore, we then explored whether miR-9-5p, an upstream regulator of DDIT4, could affect the excessive autophagy after HI injury. The results showed that LC3 II/LC3 I ratio ( $p$  < 0.01) and Beclin-1 expression ( $p$  < 0.01) were increased at 2 days following HI. MiR-9-5p mimics treatment markedly reduced LC3 II/LC3 I ratio ( $p$  < 0.01) and Beclin-1 expression ( $p$  < 0.05) compared to NC group after HI exposure (Figure 8A and B). In addition, immunofluorescence images showed strong LC3B puncta in HI exposure compared with Sham group, while miR-9-5p mimics treatment reduced HI-increased LC3B accumulation (Figure 8C). Moreover, we found that si-DDIT4 could broke the LC3 II/LC3 I ratio ( $p$  < 0.01) and Beclin-1 expression ( $p$  < 0.01) in HI-injured mice (Figure 8D and E). Meanwhile, the up-regulation of miR-9-5p expression partially rescued LC3 II/LC3 I ratio ( $p$  < 0.01) and Beclin-1 expression ( $p$  < 0.01) post HI-insult. Overexpression of DDIT4 reversed the effect of miR-9-5p mimics on HI-induced LC3 II/LC3 I ratio ( $p$  < 0.001) and Beclin-1 expression ( $p$  < 0.01) (Figure 8D and E).

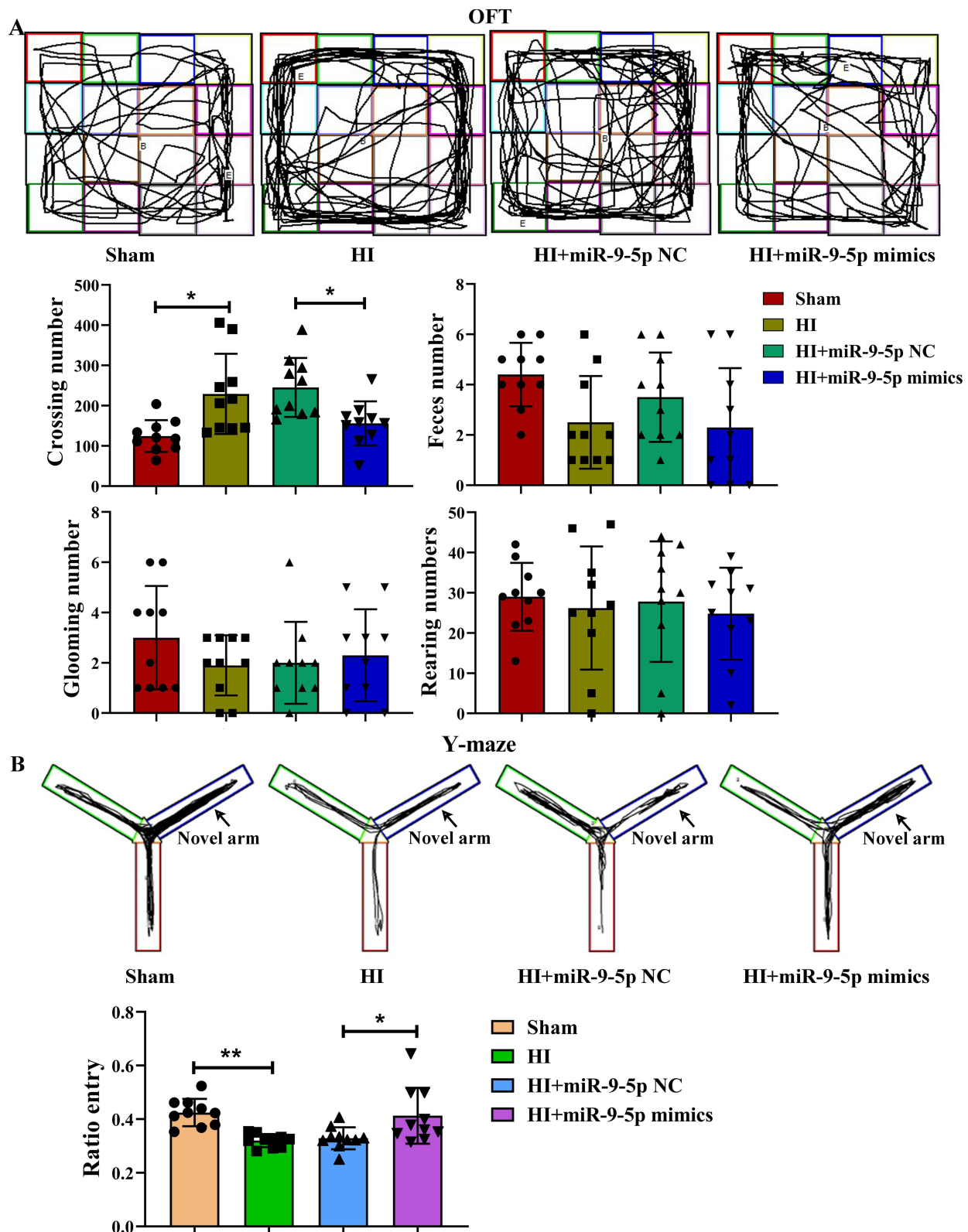
## Discussion

The aim of this study was to investigate the role of miR-9-5 in brain damage and neurobehavioral dysfunction following HI injury. Perinatal HI remains the main cause of acute brain injury in neonates and may lead to lifelong neurological dysfunction, and its pathogenesis has been extensively studied.<sup>28–30</sup> Increasing evidence supported that miRNAs dysfunction was a contributing factor for many central nervous system pathologies including stroke, traumatic brain injury and spinal cord injury.<sup>31,32</sup> Clinical studies have identified altered expressions of many miRNAs in neonatal HI



**Figure 5** MiR-9-5p up-regulated HI injury-induced down-regulation of synapse-associated protein expression. (A and B) Western blotting analysis and quantitative measurement were used to monitor protein expression levels of PSD95 and NLG-1 at 2 days post HI. (C and D) Western blotting analysis and quantitative measurement were used to examine protein expression levels of PSD95 and NLG-1 at 28 days post HI. (E) Double immunofluorescence analysis was performed with PSD95 and NeuN in Sham group, HI group, HI+miR-9-5p NC group and HI+miR-9-5p mimics group at 28 days post HI. Scale bar: 50  $\mu$ m. The data were presented as mean  $\pm$  SD, \* $p$  < 0.05, \*\*\* $p$  < 0.001 according to One-way ANOVA with Bonferroni corrections in B, D and E.

encephalopathy patients.<sup>33</sup> Further studies on miRNAs that respond to HI and their regulatory mechanisms may contribute to the development of potential targets for protection against HI injury. The present study uncovered that the expression of miR-9-5p was down-regulated after HI injury and DDIT4 might involve in the effects of miR-9-5p on HI insult in neonatal mice.



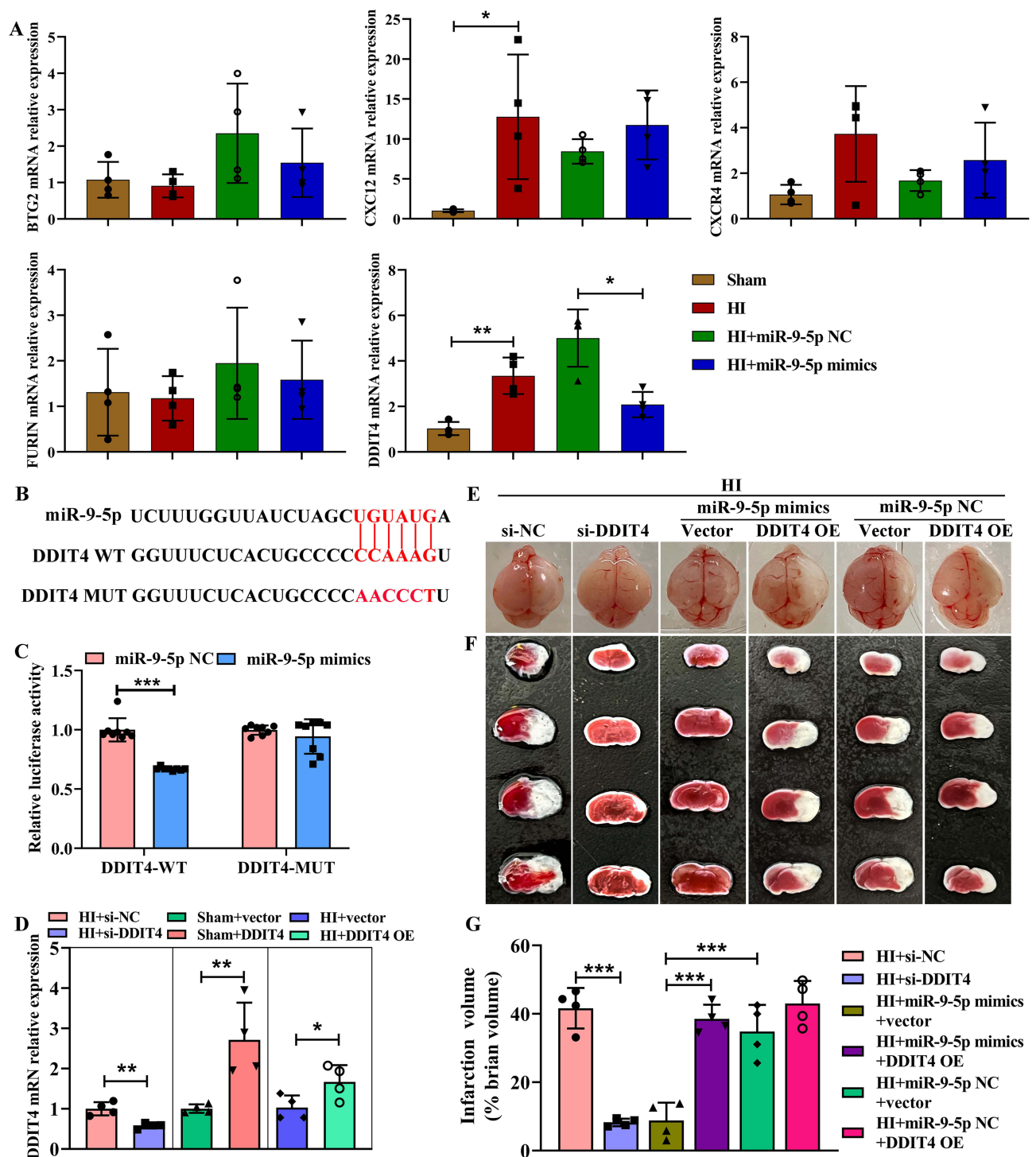


**Figure 7** Downregulation of DDIT4 expression alleviates brain injury. **(A)** Different downstream targets (BTG2, FURIN, CXCL12, CXCR4 and DDIT4) mRNA levels of miR-9-5p were detected by qRT-PCR. **(B and C)** Luciferase activity was measured in HEK293T cells transfected with DDIT4-Mut, DDIT4-WT, miR-9-5p NC and miR-9-5p mimics. **(D)** The DDIT4 mRNA level was detected after transfection with si-DDIT4, si-NC, vector, or DDIT4 overexpression (OE). **(E)** Representative brain pictures at 2 days following HI in each group treated with si-NC, si-DDIT4, miR-9-5p mimics+vector and miR-9-5p mimics+DDIT4 OE, miR-9-5p NC+vector and miR-9-5p NC+DDIT4 OE. **(F)** Example of images of TTC staining at 2 days following HI treated with si-NC, si-DDIT4, miR-9-5p mimics+vector and miR-9-5p mimics+DDIT4 OE, miR-9-5p NC+vector and miR-9-5p NC+DDIT4 OE. **(G)** Quantification of brain infarct area at 2 days following HI treated with si-NC, si-DDIT4, miR-9-5p mimics+vector and miR-9-5p mimics+DDIT4 OE, miR-9-5p NC+DDIT4 vector and miR-9-5p NC+DDIT4 OE. The data were presented as mean  $\pm$  SD,  $^{**}p < 0.01$ ,  $^{*}p < 0.05$ ,  $^{***}p < 0.001$  according to One-way ANOVA with Bonferroni corrections in **(A, C and G)**;  $^{*}p < 0.05$ ,  $^{**}p < 0.01$  according to t-test in **(D)**.

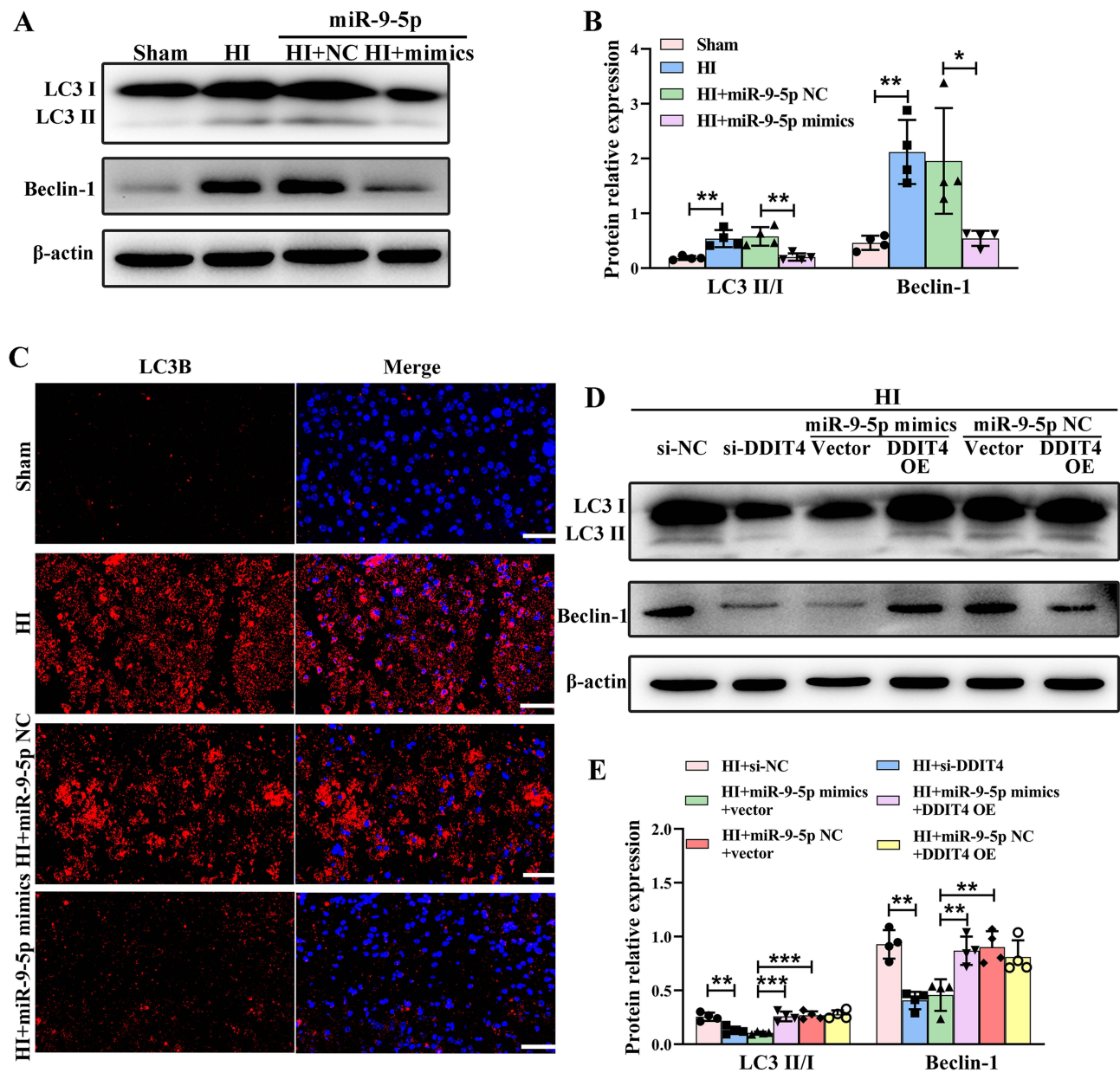


**Figure 8** Excessive autophagy after HI injury was reversed by overexpression of miR-9-5p. **(A and B)** The protein expression levels of LC3 II/LC3 I and Beclin-1 in Sham group, HI group, HI+miR-9-5p NC group and HI+miR-9-5p mimics group were determined at 2 days post HI by Western blotting. **(C)** Immunofluorescence staining of LC3B in Sham group, HI group, HI+miR-9-5p NC group and HI+miR-9-5p mimics group was determined at 2 days post HI. Scale bar: 50  $\mu$ m. **(D and E)** The protein expression levels of LC3 II/LC3 I and Beclin-1 in ipsilateral cortex following treated with si-NC, si-DDIT4, miR-9-5p mimics+vector and miR-9-5p mimics+DDIT4 OE, miR-9-5p NC +DDIT4 and miR-9-5p NC+DDIT4 OE were detected at 2 days post-HI. The data were presented as mean  $\pm$  SD. \* $p < 0.05$ , \*\* $p < 0.01$ , \*\*\* $p < 0.001$  according to One-way ANOVA with Bonferroni corrections in **(B and E)**.

MiR-9 is an ancient and highly versatile microRNA, which plays various and sometimes even opposite activities according to species and cell environment.<sup>34</sup> MiR-9-5p, highly conserved and specifically expressed in the brain, is involved in neurogenesis, neuronal regulation, and synaptic plasticity.<sup>35,36</sup> Moreover miR-9-5p has been implicated in human brain pathologies, through different specific targets, and contributed to the progression of different diseases of central nervous system. Recently study reported that oxygen and glucose deprivation-exposure up-regulated miR-9-5p expression in Neuro-2a cells, while knockdown of miR-9-5p rescued ischemic stroke-related brain damage *in vivo* and *in vitro*.<sup>37</sup> Additionally, Chi et al found that miR-9 levels were decreased in the ischemic region of stroke model, and overexpression of miR-9 by miR-9 mimics attenuated ischemic stroke,<sup>13</sup> which was consistent with the previous

study.<sup>38–41</sup> Our results revealed that miR-9-5p was down-regulated in the ipsilateral cortex of HI-injured mice, and overexpression of miR-9-5p could improve cerebral infarction, reduce brain edema and inhibit HI-induced apoptosis. These data suggested that up-regulated miR-9-5p expression might be an effective measure to alleviate brain injury caused by HI.

The inflammatory response is increasingly recognized as a major contributor to secondary neuronal injury in neonatal HI. Emerging evidence has shown that miRNAs are involved in the regulation of neuroinflammation in neonatal HI.<sup>42</sup> MiR-210 increased nuclear factor kappa-B signaling activity in HI by targeting sirtuin 1 to activate neuroinflammation in neonatal HI animals.<sup>43</sup> Down-regulation of miR-146a expression caused microglia activation and aggravated the neurobehavioral disorders in postoperative cognitive dysfunction mice.<sup>44</sup> Similar to the previous results, we found that overexpression of miR-9-5p could significantly inhibit the protein levels of pro-inflammatory factors (iNOS and IL-1 $\beta$ ), enhance the expression of anti-inflammatory factor (Arg-1), and reduce activation of microglia. Furthermore, up-regulation of miR-9-5p expression ameliorated synaptic plasticity, as well as learning and memory impairment following HI insult.

Autophagy and apoptosis are key parameters for maintaining cellular homeostasis. The interrelationship between autophagy and apoptosis is fundamental to the pathogenesis of many diseases, however, outstanding questions remain to be addressed. Many stress pathways caused autophagy and apoptosis sequentially in the same cell. Autophagy and apoptosis are cross-regulated by each other, mostly in an inhibitory manner. In specific cases, autophagy may induce apoptosis or necrosis.<sup>45,46</sup> There is a study showed that DDIT4 mediated methamphetamine-inducing autophagy stimulates apoptosis via elevating Beclin-1 expression and depleting endogenous inhibitor Bcl-2 of the cell death pathway.<sup>47</sup> In the study, blocking DDIT4 expression alleviated brain injury and down-regulated LC3 II/ LC3 I ratio and Beclin-1 expression after HI insult. Up-regulation of miR-9-5p expression targeted DDIT4 expression after HI exposure in neonatal mice, and ultimately leads to a reduced level of autophagy. Therefore, we speculated that down-regulation of miR-9-5p expression after HI injury leads to an elevated level of DDIT4, which in turn up-regulated the autophagic pathway and ultimately caused apoptosis. However, additional studies are needed to provide a definitive conclusion.

However, this study has some limitations. Firstly, our research has proved that miR-9-5p mimics treatment alleviated brain damage by inhibiting inflammation and autophagy, but we could not rule out the possibility that miR-9-5p mimics treatment may provide brain protection through other potential mechanisms. Secondly, in the present study, we examined the involvement of miR-9-5p in regulating the DDIT4 mediated autophagy pathway. However, this does not exclude the potential roles of other target genes in these signaling networks. Indeed, we postulate that other genes regulated by miR-9-5p may have various roles in the process of anti-inflammation.

In conclusion, the present study demonstrated that miR-9-5p expression was down-regulated after HI insult and overexpression of miR-9-5p could reduce neuroinflammation and apoptosis in the ipsilateral cortex, and ameliorate brain injury and neurobehavioral dysfunction. Up-regulation of miR-9-5p levels inhibited autophagy by targeting DDIT4 expression in neonatal HI ipsilateral cortex. In summary, our data clarified that overexpression of miR-9-5p negatively regulated DDIT4 expression to inhibit HI brain injury, suggested that the miR-9-5p/DDIT4 signaling pathway might be a potential target for the treatment of HI injury.

## Acknowledgments

Research funding support for this work was from the National Natural Science Foundation of China (No. 82271327, 82072535 and 81873768) to Dr. Zhen Wang. This work was supported by the Chinese Medicine Science and Technology Project of Shandong Province of China (No.M-2022123). Natural Science Foundation of Shandong Province of China (No. ZR2021MH303); the Key Research Project of Shandong Province of China (No.2018GSF118046); and the Taishan Scholar Project of Shandong Province of China (No. tsqn202103200). We thank Translational Medicine Core Facility of Shandong University for consultation and instrument availability that supported this work.

## Author Contributions

All authors made a significant contribution to the work reported, whether that is in the conception, study design, execution, acquisition of data, analysis and interpretation, or in all these areas; took part in drafting, revising or critically reviewing the article; gave final approval of the version to be published; have agreed on the journal to which the article has been submitted; and agree to be accountable for all aspects of the work.

## Disclosure

The authors report no conflicts of interest in this work.

## References

1. Douglas-Escobar M, Weiss MD. Hypoxic-ischemic encephalopathy: a review for the clinician. *JAMA Pediatr*. 2015;169(4):397–403. doi:10.1001/jamapediatrics.2014.3269
2. Ziemka-Nalecz M, Jaworska J, Zalewska T. Insights into the neuroinflammatory responses after neonatal hypoxia-ischemia. *J Neuropathol Exp Neurol*. 2017;76(8):644–654. doi:10.1093/jnen/nlx046
3. Zhou KQ, Davidson JO, Bennet L, et al. Combination treatments with therapeutic hypothermia for hypoxic-ischemic neuroprotection. *Dev Med Child Neurol*. 2020;62(10):1131–1137. doi:10.1111/dmcn.14610
4. Guo L, Zhao Y, Yang S, et al. Integrative analysis of miRNA-mRNA and miRNA-miRNA interactions. *Biomed Res Int*. 2014;2014:907420. doi:10.1155/2014/907420
5. Makeyev EV, Maniatis T. Multilevel regulation of gene expression by microRNAs. *Science*. 2008;319(5871):1789–1790. doi:10.1126/science.1152326
6. Li Y, Fan C, Wang L, et al. MicroRNA-26a-3p rescues depression-like behaviors in male rats via preventing hippocampal neuronal anomalies. *J Clin Invest*. 2021;131(16). doi:10.1172/JCI148853
7. Lai N, Wu D, Liang T, et al. Systemic exosomal miR-193b-3p delivery attenuates neuroinflammation in early brain injury after subarachnoid hemorrhage in mice. *J Neuroinflammation*. 2020;17(1):74. doi:10.1186/s12974-020-01745-0
8. Chen Y-M, He X-Z, Wang S-M, et al.  $\delta$ -opioid receptors, microRNAs, and neuroinflammation in cerebral ischemia/hypoxia. *Front Immunol*. 2020;11:421. doi:10.3389/fimmu.2020.00421
9. Cardoso AL, Guedes JR, De lima MCP. Role of microRNAs in the regulation of innate immune cells under neuroinflammatory conditions. *Curr Opin Pharmacol*. 2016;26:1–9. doi:10.1016/j.coph.2015.09.001
10. Yang D, Yu J, Liu H-B, et al. The long non-coding RNA TUG1-miR-9a-5p axis contributes to ischemic injuries by promoting cardiomyocyte apoptosis via targeting KLF5. *Cell Death Dis*. 2019;10(12):908. doi:10.1038/s41419-019-2138-4
11. Dajas-Bailador F, Bonev B, Garcez P, et al. microRNA-9 regulates axon extension and branching by targeting Map1b in mouse cortical neurons. *Nat Neurosci*. 2012;15(5):697–699. doi:10.1038/nn.3082
12. Shibata M, Nakao H, Kiyonari H, et al. MicroRNA-9 regulates neurogenesis in mouse telencephalon by targeting multiple transcription factors. *J Neurosci*. 2011;31(9):3407–3422. doi:10.1523/JNEUROSCI.5085-10.2011
13. Chi L, Jiao D, Nan G, et al. miR-9-5p attenuates ischemic stroke through targeting ERMP1-mediated endoplasmic reticulum stress. *Acta Histochem*. 2019;121(8):151438. doi:10.1016/j.acthis.2019.08.005
14. Madelaine R, Sloan SA, Huber N, et al. MicroRNA-9 couples brain neurogenesis and angiogenesis. *Cell Rep*. 2017;20(7):1533–1542. doi:10.1016/j.celrep.2017.07.051
15. Yi JH, Kwon H, Cho E, et al. REDD1 is involved in amyloid  $\beta$ -induced synaptic dysfunction and memory impairment. *Int J Mol Sci*. 2020;21(24):9482.
16. Watson A, Lipina C, McArdle HJ, et al. Iron depletion suppresses mTORC1-directed signalling in intestinal Caco-2 cells via induction of REDD1. *Cell Signal*. 2016;28(5):412–424. doi:10.1016/j.cellsig.2016.01.014
17. DeYoung MP, Horak P, Sofer A, et al. Hypoxia regulates TSC1/2-mTOR signaling and tumor suppression through REDD1-mediated 14-3-3 shuttling. *Genes Dev*. 2008;22(2):239–251. doi:10.1101/gad.1617608
18. Li Z, Zhao Q, Lu Y, et al. DDIT4 S-nitrosylation aids p38-MAPK signaling complex assembly to promote hepatic reactive oxygen species production. *Adv Sci*. 2021;8(18):e2101957. doi:10.1002/advs.202101957
19. Sun Y, Zhang J, Wang Y, et al. miR-222-3p is involved in neural tube closure by directly targeting Ddit4 in RA induced NTDs mouse model. *Cell Cycle*. 2021;20(22):2372–2386. doi:10.1080/15384101.2021.1982506
20. Zerdes I, Sifakis EG, Matikas A, et al. Programmed Death Ligand-1 gene expression is a prognostic marker in early breast cancer and provides additional prognostic value to 21-gene and 70-gene signatures in estrogen receptor-positive disease. *Mol Oncol*. 2020;14(5):951–963. doi:10.1002/1878-0261.12654
21. Lipina C, Hundal HS. Is REDD1 a metabolic éminence grise? *TEM*. 2016;27(12):868–880. doi:10.1016/j.tem.2016.08.005
22. Shoshani T, Faerman A, Mett I, et al. Identification of a novel hypoxia-inducible factor 1-responsive gene, RTP801. *Involved in Apoptosis Mol Cell Biol*. 2002;22(7):2283–2293.
23. Rice JE, Vannucci RC, Brierley JB. The influence of immaturity on hypoxic-ischemic brain damage in the rat. *Ann Neurol*. 1981;9(2):131–141. doi:10.1002/ana.410090206
24. Kim J-Y, Grunke SD, Levites Y, et al. Intracerebroventricular viral injection of the neonatal mouse brain for persistent and widespread neuronal transduction. *J Virol*. 2014;91:51863.
25. Thei L, Rocha-Ferreira E, Peebles D, et al. Extracellular signal-regulated kinase 2 has duality in function between neuronal and astrocyte expression following neonatal hypoxic-ischaemic cerebral injury. *J Physiol*. 2018;596(23):6043–6062. doi:10.1113/JP275649
26. Xu Q, Guohui M, Li D, et al. lncRNA C2dat2 facilitates autophagy and apoptosis via the miR-30d-5p/DDIT4/mTOR axis in cerebral ischemia-reperfusion injury. *Aging*. 2021;13(8):11315–11335. doi:10.18632/aging.202824

27. Ip WKE, Hoshi N, Shouval DS, et al. Anti-inflammatory effect of IL-10 mediated by metabolic reprogramming of macrophages. *Science*. 2017;356(6337):513–519. doi:10.1126/science.aal3535
28. Cai -C-C, Zhu J-H, Ye L-X, et al. Glycine protects against hypoxic-ischemic brain injury by regulating mitochondria-mediated autophagy via the AMPK pathway. *Oxid Med Cell Longev*. 2019;2019:4248529. doi:10.1155/2019/4248529
29. Li B, Concepcion K, Meng X, et al. Brain-immune interactions in perinatal hypoxic-ischemic brain injury. *Prog Neurobiol*. 2017;159:50–68. doi:10.1016/j.pneurobio.2017.10.006
30. Ham PB, Raju R, Liguori C, Fedele E, Galati S. Mitochondrial function in hypoxic ischemic injury and influence of aging. *Prog Neurobiol*. 2017;151:157. doi:10.1016/j.pneurobio.2017.01.003
31. Dewdney B, Trollope A, Moxon J, et al. Circulating MicroRNAs as biomarkers for acute ischemic stroke: a systematic review. *J Stroke Cerebrovasc Dis*. 2018;27(3):522–530. doi:10.1016/j.jstrokecerebrovasdis.2017.09.058
32. Bhalala OG, Srikanth M, Kessler JA. The emerging roles of microRNAs in CNS injuries. *Nat Rev Neurol*. 2013;9(6):328–339. doi:10.1038/nrneurol.2013.67
33. Ponnusamy V, Yip PK. The role of microRNAs in newborn brain development and hypoxic ischaemic encephalopathy. *Neuropharmacology*. 2019;149:55–65. doi:10.1016/j.neuropharm.2018.11.041
34. Coolen M, Katz S, Bally-Cuif L. miR-9: a versatile regulator of neurogenesis. *Front Cell Neurosci*. 2013;7:220. doi:10.3389/fncel.2013.00220
35. Subramanian M, Hyeon SJ, Das T, et al. UBE4B, a microRNA-9 target gene, promotes autophagy-mediated Tau degradation. *Nat Commun*. 2021;12(1):3291. doi:10.1038/s41467-021-23597-9
36. Sim S-E, Lim C-S, Kim J-I, et al. The brain-enriched MicroRNA miR-9-3p regulates synaptic plasticity and memory. *J Neurosci*. 2016;36(33):8641–8652. doi:10.1523/JNEUROSCI.0630-16.2016
37. Yan Q, Sun S-Y, Yuan S, et al. Inhibition of microRNA -9-5p and microRNA -128-3p can inhibit ischemic stroke-related cell death in vitro and in vivo. *IUBMB Life*. 2020;72(11):2382–2390. doi:10.1002/iub.2357
38. Shen B, Wang L, Xu Y, et al. Knockdown of lncRNA SNHG15 ameliorates Oxygen and Glucose Deprivation (OGD)-induced neuronal injury via regulating the miR-9-5p/TIPARP axis. *Biochem Genet*. 2022;60(2):755–769. doi:10.1007/s10528-021-10121-3
39. Nampoothiri SS, Rajanikant GK. miR-9 upregulation integrates post-ischemic neuronal survival and regeneration in vitro. *Cell Mol Neurobiol*. 2019;39(2):223–240. doi:10.1007/s10571-018-0642-1
40. Cao Y, Zhang H, Lu X, et al. Overexpression of MicroRNA-9a-5p ameliorates NLRP1 inflammasome-mediated ischemic injury in rats following ischemic stroke. *Neuroscience*. 2020;444:106–117. doi:10.1016/j.neuroscience.2020.01.008
41. Fuschi P, Maimone B, Gaetano C, et al. Noncoding RNAs in the vascular system response to oxidative stress. *Antioxid Redox Signal*. 2019;30(7):992–1010. doi:10.1089/ars.2017.7229
42. Feng X, Zhan F, Luo D, et al. LncRNA 4344 promotes NLRP3-related neuroinflammation and cognitive impairment by targeting miR-138-5p. *Brain Behav Immun*. 2021;98:283–298. doi:10.1016/j.bbi.2021.08.230
43. Li B, Dasgupta C, Huang L, et al. MiRNA-210 induces microglial activation and regulates microglia-mediated neuroinflammation in neonatal hypoxic-ischemic encephalopathy. *Cell Mol Immunol*. 2020;17(9):976–991. doi:10.1038/s41423-019-0257-6
44. Chen L, Dong R, Lu Y, et al. MicroRNA-146a protects against cognitive decline induced by surgical trauma by suppressing hippocampal neuroinflammation in mice. *Brain Behav Immun*. 2019;78:188–201. doi:10.1016/j.bbi.2019.01.020
45. Mariño G, Niso-Santano M, Baehrecke EH, et al. Self-consumption: the interplay of autophagy and apoptosis. *Nature Rev MolecCell Biol*. 2014;15(2):81–94. doi:10.1038/nrm3735
46. Noguchi M, Hirata N, Tanaka T, et al. Autophagy as a modulator of cell death machinery. *Cell Death Dis*. 2020;11(7):517. doi:10.1038/s41419-020-2724-5
47. Li B, Chen R, Chen L, et al. Effects of DDIT4 in methamphetamine-induced autophagy and apoptosis in dopaminergic neurons. *Mol Neurobiol*. 2017;54(3):1642–1660. doi:10.1007/s12035-015-9637-9

## Drug Design, Development and Therapy

Dovepress

### Publish your work in this journal

Drug Design, Development and Therapy is an international, peer-reviewed open-access journal that spans the spectrum of drug design and development through to clinical applications. Clinical outcomes, patient safety, and programs for the development and effective, safe, and sustained use of medicines are a feature of the journal, which has also been accepted for indexing on PubMed Central. The manuscript management system is completely online and includes a very quick and fair peer-review system, which is all easy to use. Visit <http://www.dovepress.com/testimonials.php> to read real quotes from published authors.

Submit your manuscript here: <https://www.dovepress.com/drug-design-development-and-therapy-journal>